Journal of Magnetic Resonance 192 (2008) 314–322

Contents lists available at ScienceDirect

Journal of Magnetic Resonance

journal homepage: www.elsevier.com/locate/jmr

The CLIP/CLAP-HSQC: Pure absorptive spectra for the measurement of one-bond couplings

Andreas Enthart [a], J. Christoph Freudenberger [a,b], Julien Furrer [a,c], Horst Kessler [a], Burkhard Luy [a,*]

[a] Munich Center for Integrated Protein Science, Department Chemie, Organische Chemie II, Technische Universität München, Lichtenbergstrasse 4, D-85747 Garching, Germany
[b] Currenta GmbH & Co. OHG, SER-ANT Spektroskopie, Geb. Q18-2, 51368 Leverkusen, Germany
[c] Institut de Chimie, Université de Neuchâtel, Avenue de Belleveaux 51, CH-2009 Neuchâtel, Switzerland

ARTICLE INFO

Article history:
Received 6 December 2007
Revised 28 February 2008
Available online 21 March 2008

Keywords:
RDCs
Partial alignment
HSQC
Pure absorption
IPAP

ABSTRACT

Heteronuclear residual dipolar one-bond couplings of organic molecules at natural abundance are most easily measured using t_2 coupled HSQC spectra. However, inevitably mismatched transfer delays result in phase distortions due to residual dispersive antiphase coherences in such experiments. In this article, slightly modified t_2 coupled HSQC experiments with clean inphase (CLIP) multiplets are introduced which also reduce the intensities of undesired long-range cross peaks. With the corresponding antiphase (CLAP) experiment, situations where α and β components overlap can be resolved for all multiplicities in an IPAP manner. A comparison of the experiments using hard pulses and shaped broadband excitation and inversion pulses on the heteronucleus is given and potential spectral artefacts are discussed in detail.

1. Introduction

Since the introduction of residual dipolar couplings (RDCs) in biomolecular NMR many experiments have been developed for the measurement of heteronuclear one-bond couplings [1–5]. Most of these experiments are designed for IS spin systems, where measurement in the indirectly acquired dimension is easily possible without loss of information and the smaller linewidths of the heteronucleus give the advantage of better defined splittings. For small- to medium-sized organic molecules, however, methylene and methyl groups must be taken into account and therefore t_2 coupled HSQC or HMQC experiments are usually used for coupling extraction in such molecules [6–9]. This kind of experiment is easily applied to isotropic samples, as the small range of one-bond heteronuclear $^1J_{CH}$ coupling constants allows the setting of close to optimal transfer delays. In partially aligned samples, nevertheless, the wide distribution of ($^1J_{CH} + D_{CH}$) couplings does not allow a correct match of the INEPT-type delays for all groups so that significant phase distortions from residual antiphase magnetization reduce the quality of the spectra (see also Fig. 1 for demonstration).

Here, several versions of HSQC experiments with purely absorptive multiplet patterns are studied that allow the direct measurement of one-bond heteronuclear couplings without phase distortions. In addition to the so-called clean inphase (clean-IP, or simply CLIP) HSQC, a second experiment resulting in absorptive antiphase (CLAP) spectra is introduced that allows the quantitative extraction of coupling constants in an α/β or IPAP-type approach. All HSQC-type experiments were implemented using either hard pulses or recently introduced BEBOP and BIBOP pulses [10,11] for excitation, inversion, and refocussing on carbon nuclei with clear advantages for the soft pulse versions.

2. Pure absorption spectra

The introduction of orienting media with sufficiently low alignment [12–14] started a surge of experimental techniques for the measurement of one-bond heteronuclear couplings, usually ($^1J_{NH} + D_{NH}$) couplings of protein amide groups. Compared to the measurement of ^{1}H, ^{15}N couplings in isotope labeled biomolecules, the measurement of ^{1}H, ^{13}C RDCs in organic molecules at natural abundance that contain CH, CH_2, and CH_3 spin systems requires pulse sequences with different abilities. A widely used approach is the acquisition of already established HSQC or HMQC experiments without heteronuclear decoupling [6–9,15]. In these experiments, couplings can be directly read from the heteronuclear splitting in the directly detected dimension. Unfortunately, the wide distribution of couplings due to the orientationally dependent D_{CH} RDCs makes the exact match of the INEPT transfer delay to $1/(2^1J_{CH} + 2D_{CH})$ impossible. Ingenious approaches like the use of adiabatic inversion pulses for compensation of chemical shift dependent spin–spin coupling effects [16] do not help, since RDCs are structurally dependent and do not scale with the chemical shift. As a result, cross peaks are significantly phase distorted as

* Corresponding author. Fax: +49 89 289 13210.
E-mail address: Burkhard.Luy@ch.tum.de (B. Luy).

1090-7807/$ - see front matter © 2008 Elsevier Inc. All rights reserved.
doi:10.1016/j.jmr.2008.03.009

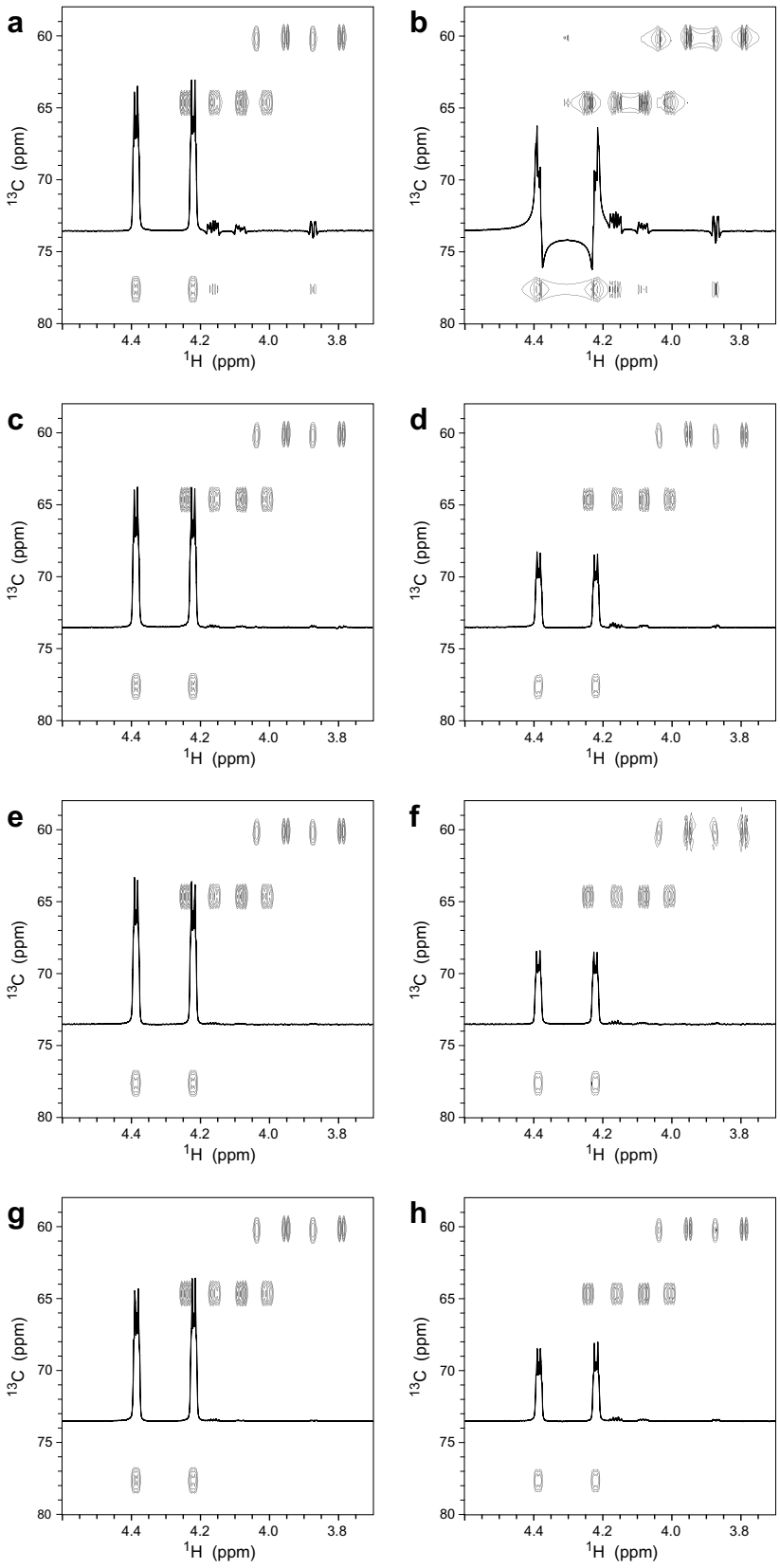

Fig. 1. Example cross peaks of t_2 coupled HSQC spectra acquired on a sample of strychnine dissolved in $CDCl_3$ using the pulse sequences shown in Fig. 2 without (a and b) and with removal of antiphase magnetization using either a phase-cycled proton 90° pulse (c and d), effective 0° and 180° pulses on carbon (e and f), or a phase-cycled 90° pulse on carbon (g and h) prior to detection. The experiments shown in Fig. 2 have been implemented with experimental delays matched to $\Delta = 1/(2 \times 150\ \text{Hz})$ (a, c, e, and g) and $\Delta = 1/(2 \times 100\ \text{Hz})$ (b, d, f, and h), respectively. Traces at 77.6 ppm are shown to demonstrate phase distortions due to mismatched delays (b) and the occurrence of long-range signals (a and b) in conventional HSQC experiments. See text for an analysis of the spectra.

shown in Fig. 1: while the multiplet at approximately 77.6 and 4.3 ppm shows a nice absorptive inphase pattern for the delay closely matched to the correct coupling of 149.2 Hz (Fig. 1a), the same signal shows strong dispersive antiphase contributions if delays are purposely mismatched by setting the delays for a heteronuclear coupling of 100 Hz (Fig. 1b). An analysis of the most basic HSQC sequence (excitation—INEPT—t_1 evolution—INEPT—detection) shows that incomplete coherence transfer from antiphase magnetization $2I_yS_z$ to inphase I_x during the INEPT step prior to detection is responsible for the observed effect: after excitation and first INEPT step antiphase magnetization evolved into $2I_zS_x \sin(\pi J\Delta)$ and chemical shift evolution during t_1 leads to a further modulation of $\exp(i\omega_S t_1)$. The second INEPT step before detection then results in the transfer

$$2I_zS_x \sin(\pi J\Delta)\exp(i\omega_S t_1) \rightarrow I_x \sin(\pi J\Delta)\exp(i\omega_S t_1)\sin(\pi J\Delta) + 2I_yS_z \sin(\pi J\Delta)\exp(i\omega_S t_1)\cos(\pi J\Delta). \quad (1)$$

For the most basic HSQC sequence this transfer function applies independent of the multiplicity of the spin system, i.e. if a CH, CH_2, or CH_3 group is present. In the ideal case the delay Δ and the coupling J are matched according to $\Delta = 1/(2J)$ where $\sin(\pi J\Delta) = 1$ and $\cos(\pi J\Delta) = 0$. For mismatched delays, however the last term of Eq. (1) leads to dispersive antiphase contributions with the corresponding undesired artefacts shown in Fig. 1.

A second, usually undesired, effect observed in conventional coupled HSQC experiment is the occurrence of cross peaks between carbons and remotely coupled protons which we would like to refer to as long-range signals in the following. Although such signals in most cases do not interfere with the measurement of heteronuclear one-bond couplings, they may overlap with direct cross peaks and lead to inaccurate coupling measurements. Long-range signals can originate from two different coherence transfers: in INEPT-type steps next to transfer via one-bond couplings, coherence transfer also occurs via heteronuclear long-range couplings with the same pathway as described in Eq. (1) with J now being the small long-range coupling. This transfer leads to mainly dispersive antiphase cross peaks due to the strong mismatch of the transfer delays. As a rule of thumb, the intensity of the long-range signals is proportional to the length and number of heteronuclear INEPT-type steps for back-transfer in a specific pulse sequence.

In addition, long-range signals can also be the result of TOCSY-type ^{1}H,^{1}H-transfer via homonuclear couplings in the strong coupling regime. Since this type of transfer also occurs if magnetization is stored along z, it is present during the whole pulse sequence and during acquisition. The exact transfer functions strongly depend on the spin system and can be quite complicated (for analytical transfer functions in the full strong coupling limit see e.g. [17–19] for isotropic, i.e. scalar coupled spins, [20] for dipolar coupled spins, and [21,22] for arbitrarily coupled spins). However, it can be stated that in addition to weak coupling evolution also homonuclear transfer of inphase magnetization occurs in the case of strongly coupled protons. While this transfer can usually be neglected during the short INEPT periods, it can result in significant $2I_z^dS_x \rightarrow 2I_z^rS_x$ transfer between the directly carbon-bound proton I^d and a remote proton I^r during t_1. If a heteronuclear $^nJ_{I^rS}$ coupling is present, a similar situation to the direct long-range signals exists and mainly dispersive antiphase cross peaks appear in HSQC spectra. Inphase transfer $I^d \rightarrow I^r$ between the two strongly coupled spins also occurs during acquisition with the consequence of inphase contributions to the long-range signals.

Both spectral artefacts, the phase distortions as well as the occurence of long-range signals, do not per se exclude measurement of heteronuclear one-bond couplings. As previously reported by Yan et al. [9], couplings can still be accurately measured as long as the multiplet components for each signal are phased separately before their distance is determined and overlap with long-range signals is rarely observed. However, phasing every multiplet component separately is a tedious process which is also very difficult to automate. As the reduction of long-range signals improves spectral quality and might prevent inaccurate $^1J_{CH}$ coupling measurements, we looked at various possibilities to remove the undesired heteronuclear dispersive antiphase magnetization prior to detection.

Three simple modifications can be added to HSQC-type experiments for antiphase removal:

(i) Addition of a proton 90° pulse prior to detection with the same phase as the detected inphase magnetization. This 90° pulse converts dispersive antiphase coherences into undetectable multi-quantum terms.
(ii) Addition of a two-step phase cycle of consecutive 90° pulses with effective 0° and 180° flip angles on carbon prior to detection which removes all heteronuclear antiphase magnetization.
(iii) The same effect is obtained by the application of a 90° pulse on carbon prior to detection which converts heteronuclear antiphase magnetization into undetectable multi-quantum coherences.

The resulting pulse sequences for a clean inphase (CLIP) HSQC experiment with coherence order selection and echo/antiecho detection scheme are shown in Fig. 2 for the three modifications for antiphase removal. For modifications (ii) and (iii) phase-cycled

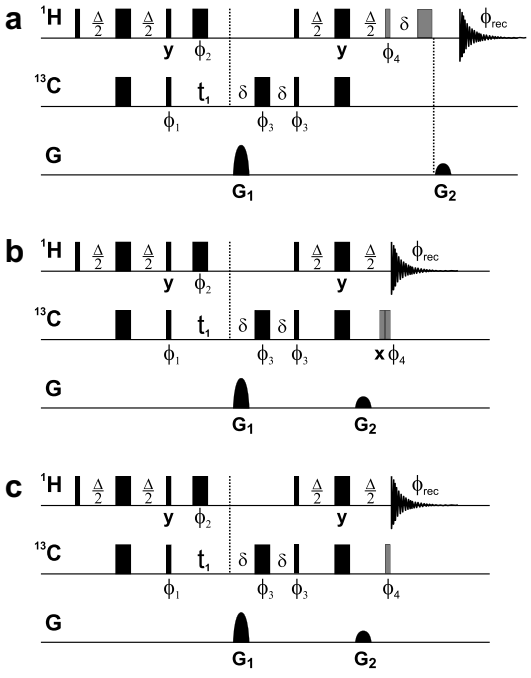

Fig. 2. CLIP-HSQC experiments for pure absorptive inphase spectra with the corresponding modifications (i)–(iii) as described in the text implemented in (a)–(c). The experiments are designed for the detection of ($^1J_{CH} + D_{CH}$) couplings at natural abundance for arbitrary multiplicities. Narrow and wide bars correspond to 90° and 180° pulses, respectively, with phase x unless indicated otherwise. The pulses added prior to detection to ensure antiphase removal are shown in gray. Phases are $\phi_1 = x, -x$, $\phi_2 = 4(x), 4(-x)$, $\phi_3 = x, x, -x, -x$, $\phi_4 = x, -x$, and $\phi_{rec} = -x, x, x, -x$. If 16 or more scans are acquired ϕ_4 can be cycled independently with $\phi_4 = 8(x), 8(-x)$. Delays should be set as close as possible to $\Delta = 1/(2 \times (^1J_{CH} + D_{CH}))$. The delay δ of typically 1 ms accommodates for the application of gradients. Coherence order selection is applied with the gradients G1 and G2 of ratio 80:20.1 for ^{13}C as the heteronucleus. Phase sensitive detection in the indirect dimension was achieved using echo–antiecho encoding on gradient G1 and phase shifting ϕ_3 and ϕ_{rec} every second increment by 180°.

carbon pulses are added to the conventional sequence as indicated by the gray bars in Fig. 2b and c. Modification (i) with proton pulse-based antiphase removal requires the coherence order selection to be placed in an additional spin echo period to avoid dephasing of the desired coherences prior to the proton 90° pulse and to ensure removal of ^{12}C-bound proton magnetization (Fig. 2a).

All three modifications efficiently remove heteronuclear antiphase magnetization as can be seen in Fig. 1c–h. However, while spectra acquired with matched delays all have a high quality appearance (Fig. 1c, e, and g), slight differences are visible in the unmatched case. Modification (ii), which was used previously in the INEPT$^+$ experiment [23], introduces a strong carbon offset dependence with the hard 180° pulse prior to detection. As can be seen in Fig. 1f, on-resonant signals (at 78 ppm) have a beautiful lineshape, but artefacts appear in cross peaks at carbon offsets of 4000 Hz (i.e. at 60 ppm) and get even worse at larger offsets (data not shown).

In modification (i) only proton pulses are added and typical offsets can easily be covered by the available hard pulses. Correspondingly, no offset dependent artefacts are visible in the spectrum, but cross peaks generally experience an undesired slight tilt in their contour shape (Fig. 1d).

In our hands best spectra are obtained with modification (iii), which has previously been used in DEPT$^+$ [23] and other pulse sequences [24–26]. The better performance compared to modification (ii) can be contributed to the robust offset dependence of the 90° pulse (see e.g. [2,27]) used for antiphase removal. Resulting lineshapes have a regular appearance (Fig. 1g) which is practically identical to the lineshapes in the spectra with matched transfer delays.

However, at offsets larger than the rf-amplitude of the carbon hard pulses, similar artefacts to the ones observed for modification (ii) appear in all spectra (data not shown). To overcome offset effects not only for the antiphase removal but also in the overall pulse sequence, we looked more closely into offset and rf-amplitude compensated shaped pulses.

3. Offset and rf-amplitude dependence

Carbon and carbon correlated spectra cover a large spectral width and at higher magnetic fields available hard pulses usually are not able to treat the whole chemical shift range equally well. Most crucial for a uniform performance of HSQC experiments are the carbon inversion pulses during both INEPT transfer steps and the refocussing pulse during coherence order encoding with ^{13}C magnetization in the transverse plane. The inclusion of offset compensated pulses like adiabatic pulses significantly improves the quality of the corresponding spectra [28–30]. The best performance, of course, is obtained if rf-amplitude and offset compensated pulses are applied for all excitation, inversion, and refocussing pulses on carbon [31]. Recently developed broadband excitation [10,32,27] and inversion [11,33] pulses based on principles of optimal control theory of spin dynamics have already proven their advantages in HSQC and HMBC-type experiments [27]. Corresponding refocussing pulses can be constructed out of BEBOP pulses using a fundamental symmetry relation [33].

The acronyms BEBOP (for excitation) and BIBOP (for inversion) each cover a whole multitude of optimized pulse shapes. For the comparison of CLIP-HSQC spectra acquired with conventional hard

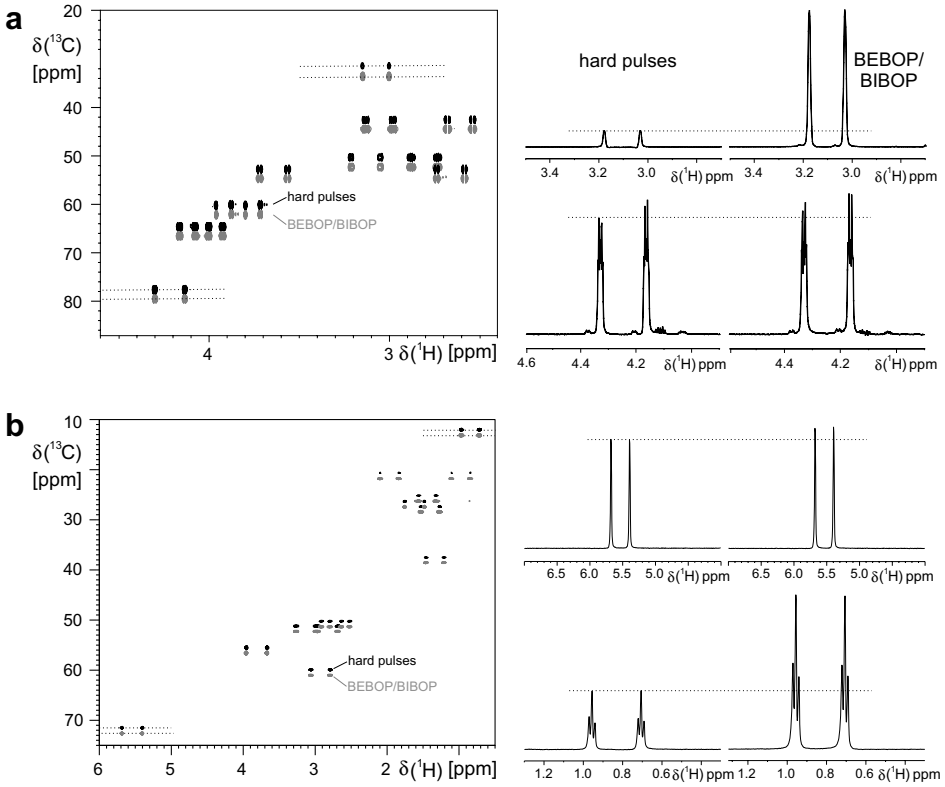

Fig. 3. Comparison of CLIP-HSQC spectra obtained using hard pulses and BEBOP/BIBOP broadband excitation and inversion pulses on ^{13}C. (a) CLIP-HSQC of strychnine in $CDCl_3$ acquired on a Bruker Avance 900 spectrometer using hard pulses with 15.6 kHz rf-amplitude (black) and phase-modulated BEBOP pulses with 1.2 ms duration and 2.4 ms 180° refocussing pulses constructed out of them with an rf-amplitude of 9.8 kHz; traces show significantly improved sensitivity for the BEBOP version with a gain of ≈9% on-resonant and ≈700% in the aliphatic region. (b) CLIP-HSQC of hydroquinidine dissolved in $CDCl_3$ acquired at 500 MHz spectrometer frequency using hard pulses with 13.2 kHz rf-amplitude (black) and BEBOP/BIBOP pulses with 337.5 μs and 307.5 μs duration and an rf-amplitude of 10 kHz; traces through corresponding signals show an increase of ≈11% on-resonant and up to ≈161% at the edges of the spectrum.

pulses and BEBOP/BIBOP pulses on carbon shown in Fig. 3a we applied 1.2 ms long PM-BEBOP (phase modulated BEBOP) pulses which work with constant rf-amplitudes between 8 and 16 kHz [27] and 180° pulses constructed out of them. At a 900 MHz spectrometer equipped with an inverse triple resonance $^{1}H,^{13}C,^{15}N$ probehead, the application of the broadband pulses leads to an increase in sensitivity of up to 700%. Any pair of pulses of the BEBOP/BIBOP families can be used for CLIP-HSQC spectra and improvements are also visible at lower spectrometer frequencies. In Fig. 3b corresponding spectra are shown at 500 MHz using arbitrarily chosen BEBOP and BIBOP pulses of 337.5 μs and 307.5 μs duration [11].

Since BEBOP pulses represent point-to-point transformations, they can only be used to transfer I_z to I_x while for the reversed transfer I_x to I_z the time-reversed pulses have to be applied. The resulting inphase CLIP-HSQC pulse sequence is shown in Fig. 4a with the corresponding shaped pulses indicated.

4. Multiplet reduction

The CLIP-HSQC, even more so when using broadband and rf-compensated BEBOP/BIBOP pulses, results in pure absorptive spectra of high quality. However, frequently overlapping signals are encountered especially in CH_2 groups where the two proton resonances are correlated with the identical carbon frequency. An example is shown in Fig. 5 for a methylene group of 6-methyl-2-phenyl-1-oxa-spiro[4,4]non-2-en-4-one [34,35]. The two cross peaks in this case could be resolved by either changing the spectrometer frequency or e.g. by applying spin state selective or IPAP-type experiments [1–3,8], on which we will concentrate in the following.

Among the wealth of pulse sequences the so-called HSQC-α/β [2] is most easily applied to arbitrary heteronuclear spin systems, i.e. CH, CH_2, and CH_3 groups. By acquiring inphase and antiphase terms during acquisition in two otherwise identical experiments, the addition/subtraction of the resulting spectra separates α and β multiplet components in two subspectra that avoid overlap due

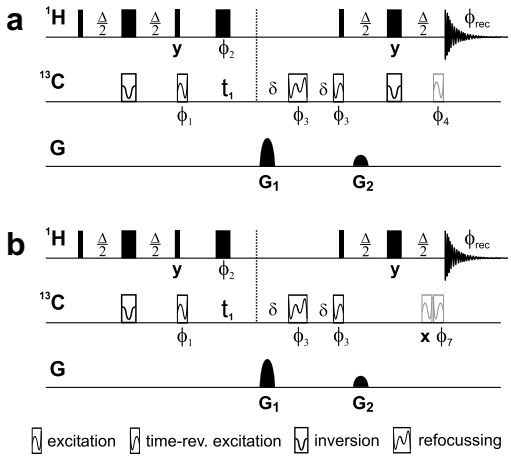

Fig. 4. Clean inphase (CLIP) and clean antiphase (CLAP) HSQC pulse sequences using broadband excitation and inversion pulses on ^{13}C. The icons corresponding to inversion, excitation, time-reversed excitation, and refocussing pulses are explained at the bottom of the figure. The refocussing pulse can be constructed out of two excitation pulses as described in [33]. (a) Phases, delays, and gradients of the broadband version of the CLIP-HSQC are identical to the hard pulse version shown in Fig. 2. The broadband excitation pulse for removal of antiphase coherences is drawn in gray. (b) The CLAP-HSQC has the same basic setup as the CLIP-HSQC with additional phase $\phi_7 = x, x, -x, -x$ and receiver phase $\phi_{rec} = y, -y$. The two excitation pulses drawn in gray for effective 0°/180° cycling ensure that only antiphase coherences are detected. Since inphase contributions to the spectrum are typically quite small, the pulses can be removed (with receiver phase then $\phi_{rec} = y, -y, -y, y$) without significant change in spectral quality.

to the reduction of multiplet areas in the subspectra. The corresponding clean inphase (CLIP) and antiphase (CLAP) pulse sequences are shown in Fig. 4a and b (note that the antiphase spectrum can also be recorded later on after a quick inspection of the initial inphase spectrum has revealed potentially insufficient resolution). A sensitivity enhanced version for inphase and antiphase spectra has recently been published by Nolis et al. [8], but signal intensities in this case significantly differ for CH, CH_2, and CH_3 groups and depend on the mismatch for both delays Δ and Δ' used for the $I_zS^- \rightarrow I^-/2I^-S_z$ transfer. Since also long-range signals increase with the extended back-transfer and no satisfying universal rotation broadband 90° pulse for covering the complete ^{13}C chemical shift range is yet available, we decided to go for the CLAP-HSQC without sensitivity enhancement. As can nicely be seen in Fig. 5, the separation of multiplet components after addition/subtraction of the two resulting spectra allows the measurement of $(^{1}J_{CH} + D_{CH})$ couplings even if signals show severe overlap in the CLIP-HSQC.

The CLIP/CLAP approach leads to very good subtraction results as long as the delays for the back-transfer in the CLIP-HSQC match approximately with the actual heteronuclear one-bond couplings. Since the "coherence transfer" in the CLAP-HSQC is only determined by 90° pulses independent of applied delays (i.e. effectively the transfer described in Eq. (1) does not occur), its signal intensity can be assumed to be 100% while for the CLIP-HSQC transfer it is scaled relative to the CLAP case by $\kappa = \sin\pi(^{1}J_{CH} + D_{CH})\Delta$ (cf. Eq. (1)). If the heteronuclear one-bond coupling deviates from the nominal coupling of the delay, e.g. by ±10%, ±20%, and ±30%, the resulting α and β subspectra contain addition/subtraction errors on the order of 1.2%, 5%, and 11%, respectively. Such errors are of very minor importance for coupling measurements as long as the multiplet components are not overlapped, which should be the case for the majority of signals. The few overlapped signals, however, have to be corrected individually in order to assure accurate coupling determination. Fig. 6 shows α and β subspectra obtained for hydroquinidine using the CLIP/CLAP approach. Traces for various signals indicate the dependence of addition/subtraction errors on the nominal coupling used for setting the delay. By scaling the CLAP spectrum according to κ with the actual delay Δ used in the experiment and the estimated coupling of the particular cross peak of interest, the resulting addition/subtraction errors in the α and β subspectra are significantly reduced and more accurate coupling measurements are possible. In cases where the α component of one signal overlaps with the β component of a second signal (Figs. 5 and 6c), the CLAP spectra have to be scaled individually to obtain the minimal possible addition/subtraction errors in the corresponding α and β subspectra.

5. Experimental

The presented CLIP and CLAP-HSQC experiments have been used extensively in our laboratory to obtain heteronuclear one-bond scalar and residual dipolar couplings from organic molecules at natural abundance. Several of the obtained spectra have already been published as t_2 coupled HSQC spectra as, for example, all spectra shown in [14,36]. The spectra shown in this article were recorded on isotropic samples to specifically characterize the properties of the CLIP/CLAP approach. Since the heteronuclear Hamiltonians for scalar and dipolar couplings are of the same form, the results shown here can be directly transferred to partially aligned samples.

Conventional and CLIP-HSQC spectra with and without sensitivity enhancement and delays matched to nominal J-values of 100 Hz, 150 Hz, and 200 Hz have been recorded for strychnine dissolved in $CDCl_3$ with 16,384 × 256 data points, 4 scans per increment, and spectral widths of 130.0 ppm (^{13}C) and 13.0 ppm (^{1}H)

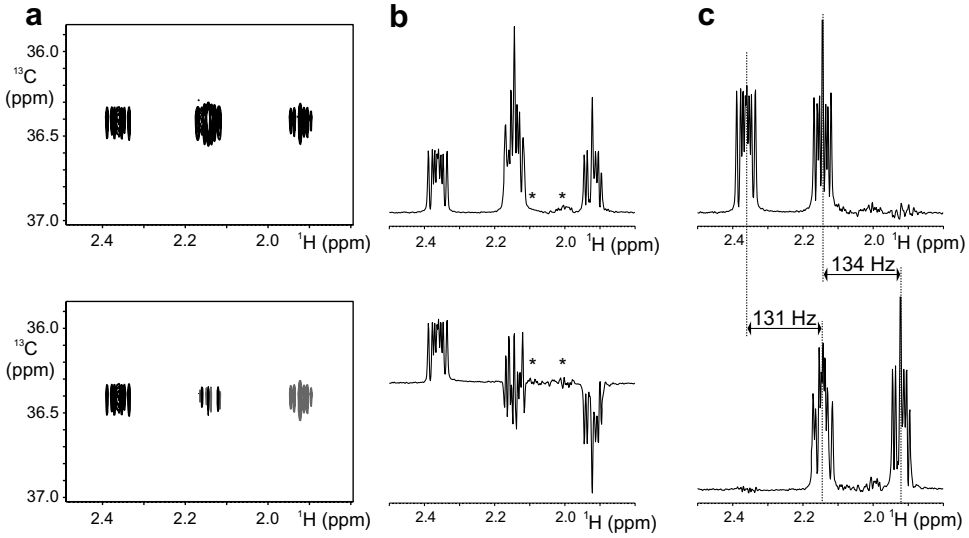

Fig. 5. CLIP and CLAP-HSQC spectra of a methylene group of 6-methyl-2-phenyl-1-oxa-spiro[4,4]non-2-en-4-one [34,35] dissolved in $CDCl_3$ and recorded at 600 MHz proton frequency (a). After combining the two spectra in IPAP manner (b), coupling constants of the overlapped signals can be determined from the corresponding α and β subspectra (c). Residual long-range signals are marked with asterisks in (b).

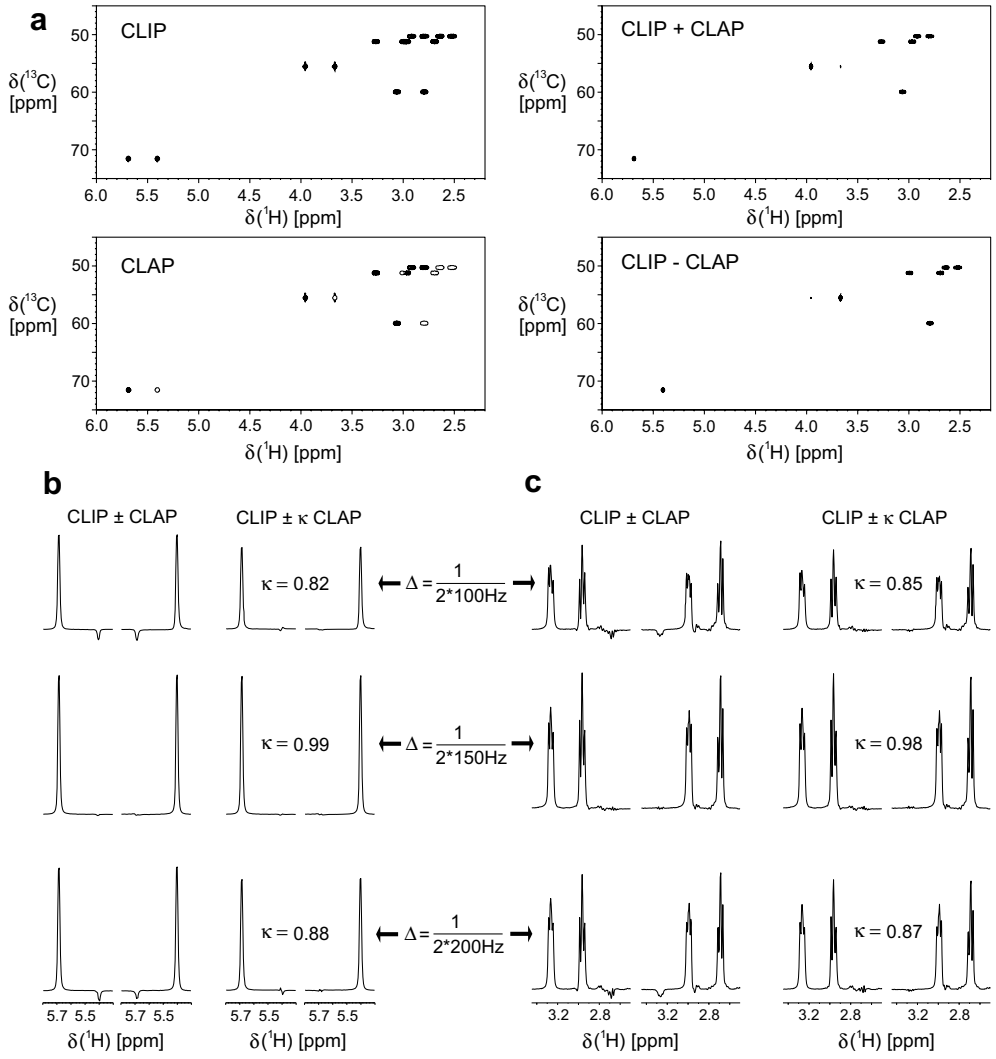

Fig. 6. CLIP and CLAP-HSQC recorded on hydroquinidine in $CDCl_3$ are added/subtracted to obtain subspectra with only α or β multiplet components (a). Traces at 71.5 ppm (b) and 51.0 ppm (c) for the two subspectra are shown for various delays Δ using either direct or corrected addition/subtraction of CLIP and CLAP-HSQC spectra. For the correction the scaling factor $\kappa = \sin\pi\,(^{1}J_{CH} + D_{CH})\Delta$ is applied to the CLAP-HSQC spectra for the corresponding couplings of 139 Hz (b) and 135 Hz (c), respectively, which leads to cleaner subspectra and more accurate coupling constant determination from overlapped signals.

on a Bruker Avance 900 spectrometer. Spectra for comparing hard pulse and BEBOP/BIBOP versions of the CLIP-HSQC were obtained on a Bruker Avance 900 spectrometer equipped with a room temperature $^{1}H,^{13}C,^{15}N$-TXI triple resonance probehead using the strychnine sample (8192×512 data points with spectral widths of 13.1 ppm (11,792 Hz) and 122.7 ppm (27,778 Hz)) and on a Bruker Avance 500 spectrometer with equivalent probehead using a 400 mM sample of hydroquinidine dissolved in $CDCl_3$ (8192×768 data points with spectral widths of 10 ppm (5000 Hz) and 160 ppm (20,116 Hz)) and a 500 mM sample of sucrose dissolved in D_2O (8192×512 data points with spectral widths of 12.02 ppm (6009.6 Hz) and 39.77 ppm (5000 Hz)). Hard pulses and BEBOP/BIBOP pulses were applied as described in Fig. 3. The 500 MHz setup with BEBOP/BIBOP pulses was also used for the evaluation of the CLIP/CLAP addition/subtraction approach, again varying the nominal J-values for the delay Δ to 100 Hz, 150 Hz, and 200 Hz. CLIP/CLAP-HSQC spectra on the spiro compound (Fig. 5) were acquired on a Bruker DMX600 spectrometer with 8192×1024 data points and spectral widths of 70 ppm (^{13}C) and 8 ppm (^{1}H). All spectra were apodized using 90°-shifted quadratic sine functions in both dimensions.

6. Discussion

In this article we have put together very basic pulse sequences designed for robust, pure absorptive detection of ($^{1}J_{CH} + D_{CH}$) couplings at natural abundance. The main element for improved spectral quality is the removal of heteronuclear antiphase magnetization prior to detection, for which three pulse sequence modifications have been studied in detail. Modification (iii), a phase-cycled 90 degree pulse on carbon prior to detection, results in spectra of highest quality. In this case, a single $90°_x$ pulse without phase cycling already transfers $2I_yS_z$ to unobservable $2I_yS_y$ coherences and the ± phase cycling additionally ensures the removal of possibly present $2I_yS_y$-terms that would be transferred to detectable $-2I_yS_z$ coherence by the $90°_x$ pulse.

The presented experiments are designed to obtain spectra with as few as possible artefacts. In our hands least distortions are obtained in experiments without sensitivity enhancement. This, of course, comes at the expense of reduced signal intensity. If sample concentration is limited and highest possible sensitivity is required, the recently published set of inphase and antiphase experiments [8], perhaps in combination with a sensitivity enhanced version of the CLIP-HSQC, should be preferred as long as the one-bond coupling variation is not too strong. In cases with significant variations in coupling constants, as e.g. in partially aligned samples containing simultaneously aromatic and aliphatic signals of different multiplicities, the advantage in signal-to-noise of sensitivity enhanced experiments is lost due to the inevitable mismatch of delays. The CLIP-HSQC without sensitivity enhancement benefits also from the single coherence transfer function derived in Eq. 1 for all CH, CH_2, and CH_3 groups, since coupling evolution only takes place with protons in the transverse plane. The IPAP-type approach with addition of scaled antiphase spectra (see Fig. 6) therefore is generally applicable using the given scaling function and complex scaling factors for the different multiplicities, as would be the case for a sensitivity enhanced HSQC [8], can be avoided.

It must be clearly stated that none of the pulse sequences introduced do remove phase artefacts originating from $^{1}H,^{1}H$ couplings. As can be seen in previously published experimental slices of e.g. [37,8] this is a problem especially for CH_2 groups with large $^{2}J_{HH}$ couplings. The evolution of $^{1}H,^{1}H$ couplings can in principle be avoided by the use of CPMG-type transfer steps [38–40,26], but this would limit the affordable bandwidth of the proposed experiments and therefore was not persued here. In experiments without back-transfer delays, as e.g. the case in the P.E.HSQC [41], cleanest spectra can be obtained by the use of a zero quantum suppression scheme [41,42], which, in principle, could also be added as an additional filter to the presented CLIP/CLAP-HSQC experiments. However, since the presented experiments do not use sensitivity enhancement schemes, $^{1}H,^{1}H$ couplings effectively only evolve during the short back-transfer period and practically no distortions are visible in the resulting spectra. Only in cases with very large D_{HH} RDCs significant phase distortions will occur.

As demonstrated previously, BEBOP and BIBOP pulses as broadband shaped pulses of very high quality applied to uniformly cover the ^{13}C chemical shift range give clearly visible improvements in performance compared to conventional hard pulses. Especially for organic molecules with long relaxation times the pulse shapes of durations in the hundred microseconds to low millisecond range promise significant enhancements in practically all heteronuclear experiments. In the pulse sequence, of course, other offset and B_1-field inhomogeneity compensated excitation and inversion pulses can be used, although BEBOP and BIBOP pulses have been shown to usually outperform other pulse shapes [11]. Nevertheless, while BIBOP pulses can be implemented on most consoles in the same way as more conventional pulse shapes, BEBOP pulses impose high demands on electronics which only recent spectrometer consoles with linearized amplifiers and fast switching times can fulfill. In such cases it might be worth considering composite pulses or even a hard 90° as the better solution. On Bruker Avance spectrometers with SGU units for frequency generation the implementation of the pulse shapes did not lead to any problems.

The suppression of long-range signals is partially achieved in the CLIP/CLAP-HSQC spectra. While the CLIP-HSQC only contains the very minor inphase component of direct cross peaks due to heteronuclear long-range coupling evolution, the CLAP-HSQC retains the stronger antiphase components. Long-range signals originating from homonuclear strong coupling evolution are present in both experiments (as in all HSQC/HMQC-type experiments).

Long-range artefacts in general influence the heteronuclear one-bond signal patterns and may lead to significant errors in coupling constant determination as is demonstrated in Fig. 7: the equivalent slices of a CLIP-HSQC and a corresponding conventional coupled HSQC recorded on a sucrose sample have been used to extract coupling constants by either directly shifting the multiplet components relative to each other (in the case of the CLIP-HSQC) or by phasing each multiplet component separately to absorption as described in more detail in [9]. Without linebroadening, both methods lead to the identical one-bond coupling constant of 144.8 Hz, which deviates only by 5.2 Hz from the nominal coupling of 150 Hz used for setting the INEPT delays. With linebroadening added to simulate e.g. partially aligned samples, overlap with the neighboring long-range cross peak leads to significant measurement errors, which are up to 3.6 Hz for 25 Hz linebroadening in the conventional coupled HSQC. The CLIP-HSQC still contains the strong coupling-based component of the long-range cross peak, but the overall intensity of this unwanted signal is much lower compared to the conventional HSQC and resulting errors in coupling constant measurement are considerably reduced. The best way to extract coupling constants in the presence of strong coupling artefacts is, of course, the simulation and fitting of the spectrum using the whole spin system. For broad lines, however, this can only be achieved if homonuclear couplings can be estimated from other experiments. As a remark, it should be noted that dipolar D_{HH} couplings lead to different effective Hamiltonians compared to the equivalent J_{HH} scalar couplings ([21,22] and basic NMR-literature like [44]). This must be taken into account for the potential fitting procedure.

Finally we would like to mention that the high spectral quality of CLIP-HSQC spectra may, in principle, allow the automated extraction of heteronuclear one-bond coupling constants. But as

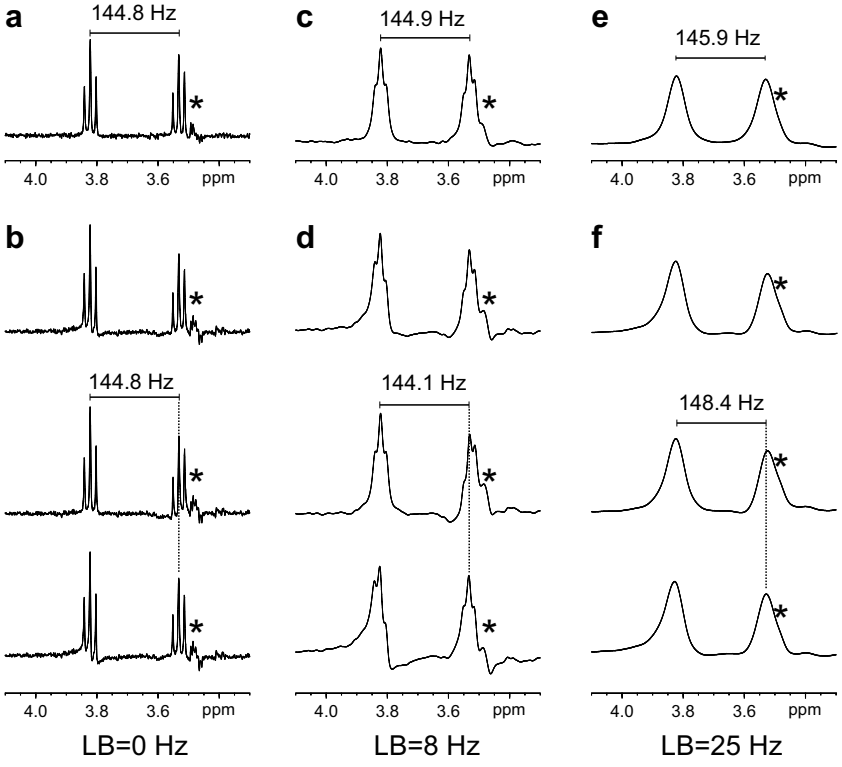

Fig. 7. Traces of the H3′–C3′ signal (following the nomenclature used in [14]) at 3.68 (^{1}H) and 72.5 ppm (^{13}C) of sucrose dissolved in D_2O acquired using the CLIP-HSQC shown in Fig. 2c (a, c, and e) and a conventional coupled HSQC sequence (b, d, and f) which corresponds to the CLIP-HSQC without the 90° pulse prior to detection. The long-range signal to the neighboring H2′ is indicated by an asterisk. Delays for coherence transfer were set to $\Delta = 1/(2 \times 150\ \text{Hz})$. Coupling constants were extracted by shifting the individual multiplet components until lineshapes fitted best in the case of the CLIP-HSQC, and by phasing the left (b, d, and f center) and right (b, d, and f bottom) multiplet component individually into absorption before the actual measurement as described in [9]. While identical coupling constants are determined for the signals processed without linebroadening (a and b), processing with additional exponential linebroadening (LB) of 8 Hz (c and d) and 25 Hz (e and f) leads to overlap with the long-range signal and subsequently to errors in coupling measurement. Errors are largest for the conventional coupled HSQC with individual phase correction and for strongest linebroadening. The linebroadening has been added to simulate the complex multiplet patterns arising in spectra of partially oriented samples (see e.g. [13,43].

discussed above, strong coupling artefacts or signal overlap might lead to significant errors and visual inspection of cross peaks is certainly recommended. The IPAP-type approach shown in Fig. 6 involves reprocessing of individual peaks and would be applied manually for the few signals with corresponding overlap pattern.

7. Conclusion

Variants of t_2 coupled HSQC experiments with improved spectral appearance for the extraction of heteronuclear ($^1J_{CH} + D_{CH}$) couplings are introduced: residual heteronuclear antiphase coherences that are responsible for phase distortions in conventional t_2 coupled HSQC experiments can simply be removed by a phase-cycled carbon 90° pulse directly before acquisition. The same pulse sequence element also strongly reduces artefactual long-range cross peaks that are decoupled in conventional HSQC experiments. Equivalent to the previously introduced α/β-HSQC, inphase and antiphase spectra in pure absorption are used to separate multiplet components in different subspectra for improved resolution and a simple scaling procedure for the reduction of addition/subtraction artefacts is introduced. Additional improvement in spectral quality is obtained by the use of high quality broadband pulses like members of the BEBOP/BIBOP pulse family. The presented pulse sequences have been successfully applied to a large variety of isotropic and partially aligned samples in our laboratory, leading generally to spectra with very few artefacts and good interpretability.

Pulse sequences in Bruker Avance format and selected data sets will be available online for download at http://www.org.chemie.tu-muenchen.de/people/bulu.

Acknowledgments

B.L. thanks the Fonds der Chemischen Industrie and the DFG for financial support (Emmy Noether fellowship LU 835/1). We thank Stefan F. Kirsch, Clémence Liébert, and Helge Menz (Technical University Munich, Germany) for kindly providing valuable spiro compounds. We would also like to thank Christina M. Thiele (University of Darmstadt, Germany) for helpful discussions.

References

[1] M.D. Sørensen, A. Meissner, O.W. Sørensen, Spin-state-selective coherence transfer via intermediate states of two-spin coherence in IS spin systems application to E.COSY-type measurement of J coupling constants, J. Biomol. NMR 10 (1997) 181–186.
[2] P. Andersson, J. Weigelt, G. Otting, Spin-state selection filters for the measurement of heteronuclear one-bond coupling constants, J. Biomol. NMR 12 (1998) 435–441.
[3] M. Ottiger, F. Delaglio, A. Bax, Measurement of J and dipolar couplings from simplified two-dimensional NMR spectra, J. Magn. Reson. 131 (1998) 373–378.
[4] M.D. Sørensen, A. Meissner, O.W. Sørensen, ^{13}C natural abundance S^3E and S^3CT experiments for measurement of J coupling constants between $^{13}C\alpha$ or $^1H\alpha$ and other protons in a protein, J. Magn. Reson. 137 (1999) 237–242.
[5] B. Luy, J.P. Marino, JE-TROSY: combined J- and TROSY-spectroscopy for the measurement of one bond couplings in macromolecules, J. Magn. Reson. 163 (2003) 92–98.
[6] P. Permi, A spin-state-selective experiment for measuring heteronuclear one-bond and homonuclear two-bond couplings from an HSQC-type spectrum, J. Biomol. NMR 22 (2002) 27–35.
[7] T. Parella, M. Gairí, Simultaneous recording of spin-state-selective NMR spectra for different I_nS spin systems, J. Am. Chem. Soc. 126 (2004) 9821–9826.
[8] P. Nolis, J.F. Espinosa, T. Parella, Optimum spin-state selection for all multiplicities in the acquisition dimension of the HSQC experiment, J. Magn. Reson. 180 (2006) 39–50.

[9] J.L. Yan, A.D. Kline, H.P. Mo, M.J. Shapiro, E.R. Zartler, A novel method for the determination of stereochemistry in six-membered chairlike rings using residual dipolar couplings, J. Org. Chem. 68 (2003) 1786–1795.
[10] T. Skinner, T. Reiss, B. Luy, N. Khaneja, S.J. Glaser, Application of optimal control theory to the design of broadband excitation pulses for high resolution NMR, J. Magn. Reson. 163 (2003) 8–15.
[11] K. Kobzar, T. Skinner, N. Khaneja, S.J. Glaser, B. Luy, Exploring the limits of broadband excitation and inversion pulses, J. Magn. Reson. 170 (2004) 236–243.
[12] A. Bax, Weak alignment offers new NMR opportunities to study protein structure and dynamics, Protein Science 12 (2003) 1–16.
[13] B. Luy, K. Kobzar, S. Knör, D. Heckmann, J. Furrer, H. Kessler, Orientational properties of stretched poly(styrene) gels in various organic solvents and the suppression of its residual ^{1}H-NMR signals, J. Am. Chem. Soc. 127 (2005) 6459–6465.
[14] Kummerlöwe, J. Auernheimer, A. Lendlein, B. Luy, Stretched poly(acrylnitrile) as a scalable alignment medium for DMSO, J. Am. Chem. Soc. 129 (2007) 6080–6081.
[15] B. Luy, K. Kobzar, H. Kessler, Easy and scalable method for the partial alignment of organic molecules for measuring residual dipolar couplings, Angew. Chem., Int. Ed. 43 (2004) 1092–1094.
[16] Ē. Kupče, R. Freeman, Compensation for spin–spin coupling effects during adiabatic pulses, J. Magn. Reson. 127 (1997) 36–48.
[17] L. Braunschweiler, R.R. Ernst, Coherence transfer by isotropic mixing: application to proton correlation spectroscopy, J. Magn. Reson. 53 (1983) 521.
[18] O. Schedletzky, S.J. Glaser, Analytical coherence-transfer functions for the general AMX spin system under isotropic mixing, J. Magn. Reson. A 123 (1996) 174–180.
[19] B. Luy, S.J. Glaser, Analytical polarization transfer functions for four coupled spins $\frac{1}{2}$ under isotropic mixing conditions, J. Magn. Reson. 138 (1999) 19–27.
[20] B. Luy, S.J. Glaser, Analytical polarization and coherence transfer functions of three dipolar coupled spins $\frac{1}{2}$, J. Magn. Reson. 142 (2000) 280–287.
[21] D.M. Taylor, A. Ramamoorthy, Analysis of dipolar-coupling-mediated coherence transfer in a homonuclear two spin-$\frac{1}{2}$ solid-state system, J. Magn. Reson. 141 (1999) 18–28.
[22] B. Luy, S.J. Glaser, Superposition of scalar and residual dipolar couplings: analytical transfer functions for three spins $\frac{1}{2}$ under cylindrical mixing conditions, J. Magn. Reson. 148 (2001) 169–181.
[23] O.W. Sørensen, R.R. Ernst, Elimination of spectral distortion in polarization transfer experiments. Improvements and comparison of techniques, J. Magn. Reson. 51 (1983) 477–489.
[24] W. Kozminski, Simplified multiplet pattern HSQC-TOCSY experiment for accurate determination of long-range heteronuclear coupling constants, J. Magn. Reson. 137 (1999) 408–412.
[25] T. Parella, J. Belloc, Spin-state-selective excitation in selective 1D inverse NMR experiments, J. Magn. Reson. 148 (2001) 78–87.
[26] K. Kobzar, B. Luy, Analyses, extensions and comparison of three experimental schemes for measuring ($^{n}J_{CH} + D_{CH}$)-couplings at natural abundance, J. Magn. Reson. 186 (2007) 131–141.
[27] T.E. Skinner, K. Kobzar, B. Luy, R. Bendall, W. Bermel, N. Khaneja, S.J. Glaser, Optimal control design of constant amplitude phase-modulated pulses: application to calibration-free broadband excitation, J. Magn. Reson. 179 (2006) 241–249.
[28] K. Hallenga, G.M. Lippens, A constant-time ^{13}C–^{1}H HSQC with uniform excitation over the complete ^{13}C chemical shift range, J. Biomol. NMR 5 (1995) 59–66.
[29] P.C.M. van Zijl, T.-L. Hwang, M. O'Neil Johnson, M. Garwood, Optimized excitation and automation for high-resolution NMR using B_1-insensitive rotation pulses, J. Am. Chem. Soc. 118 (1996) 5510–5511.
[30] C. Zwahlen, P. Legault, S.J.F. Sébastien, J.F. Vincent, J. Greenblatt, R. Konrat, L.E. Kay, Methods for measurement of intermolecular NOEs by multinuclear NMR spectroscopy: application to a bacteriophage λ N-peptide/*boxB* RNA complex, J. Am. Chem. Soc. 119 (1997) 6711–6721.
[31] G.S. Armstrong, K.E. Cano, V.A. Mandelshtam, A.J. Shaka, B. Bendiak, Rapid 3D NMR using the filter diagonalization method: application to oligosaccharides derivatized with ^{13}C-labeled acetyl groups, J. Magn. Reson. 170 (2004) 156–163.
[32] T.E. Skinner, T.O. Reiss, B. Luy, N. Khaneja, S.J. Glaser, Reducing the duration of broadband excitation pulses using optimal control with limited RF amplitude, J. Magn. Reson. 167 (2004) 68–74.
[33] B. Luy, K. Kobzar, T.E. Skinner, N. Khaneja, S.J. Glaser, Construction of universal rotations from point to point transformations, J. Magn. Reson. 176 (2005) 179–186.
[34] S.F. Kirsch, J.T. Binder, B. Crone, A. Duschek, T.T. Haug, C. Liébert, H. Menz, catalyzed tandem reaction of 3-silyloxy-1,5-enynes consisting of cyclization and pinacol rearrangement, Angew. Chem., Int. Ed. 46 (2007) 2310–2313.
[35] J.T. Binder, B. Crone, S.F. Kirsch, C. Liébert, H. Menz, Synthesis of heterocyclic ring systems by transition-metal-catalyzed cyclization–migration reactions—a diversity-oriented strategy for the construction of spirocyclic 3(2H)-furanones and 3-pyrrolones, Eur. J. Org. Chem. (2007) 1636–1647.
[36] J. Klages, C. Neubauer, M. Coles, H. Kessler, B. Luy, Structure refinement of cyclosporin A in chloroform using RDCs measured in a stretched PDMS-Gel, ChemBioChem 6 (2005) 1672–1678.
[37] M. Sattler, J. Schleucher, O. Schedletzky, S.J. Glaser, C. Griesinger, N.C. Nielsen, O.W. Sørensen, α & β HSQC an HSQC-type experiment with improved resolution for I_2S groups, J. Magn. Reson. A 119 (1996) 171–179.
[38] B. Luy, J.P. Marino, ^{1}H–^{31}P CPMG-correlated experiments for the assignment of nucleic acids, J. Am. Chem. Soc. 123 (2001) 11306–11307.
[39] H. Koskela, I. Kilpelainen, S. Heikkinen, LR-CAHSQC: an application of a Carr–Purcell–Meiboom–Gill-type sequence to heteronuclear multiple bond correlation spectroscopy, J. Magn. Reson. 164 (2003) 228–232.
[40] K.E. Kövér, G. Batta, K. Fehér, Accurate measurement of long-range heteronuclear coupling constants from undistorted multiplets of an enhanced CPMG-HSQMBC experiment, J. Magn. Reson. 181 (2006) 89–97.
[41] P. Tzvetkova, S. Simova, B. Luy, P.E.HSQC: a simple experiment for simultaneous and sign-sensitive measurement of ($^{1}J_{CH} + D_{CH}$) and ($^{2}J_{HH} + D_{HH}$) couplings, J. Magn. Reson. 186 (2007) 193–200.
[42] M.J. Thrippleton, J. Keeler, Elimination of zero-quantum interference in two-dimensional NMR spectra, Angew. Chem., Int. Ed. 42 (2003) 3938–3941.
[43] J.C. Freudenberger, S. Knör, K. Kobzar, D. Heckmann, T. Paululat, H. Kessler, B. Luy, Stretched polyvinylacetate-gels as NMR-alignment media for the measurement of residual dipolar couplings in polar organic solvents, Angew. Chem., Int. Ed. 44 (2005) 423–426.
[44] M.H. Levitt, Spin Dynamics Basics of Nuclear Magnetic Resonance, Wiley, New York, 2001.